

Computer Aided Diagnosis (CAD) for mammography with Markov Random Field method with Simulated Annealing optimization

Ni Larasati Kartika Sari¹, Prawito Prajitno², Lukmanda Evan Lubis², and Djarwani Soeharso Soejoko²

¹Universitas Nasional, Jakarta, Indonesia 12520

²Universitas Indonesia, Depok, West Java, Indonesia 16424

E-mail: tikpo09@gmail.com

Received August 02 2017

Revised August 31 2017

Accepted for publication September 02 2017

Published September 04 2017

Abstract: Mammography is the most effective technique to detect breast abnormalities. In most cases, mammograms are evaluated by radiologists. However, diagnosis performed radiologist has a lot of limitations. Computer Aided Diagnosis (CAD) with various methods had been developed to help radiologist in evaluating mammograms. This research developed CAD for mammography based on image segmentation using Markov Random Field with Simulated Annealing optimization (MRF/SA). We combined MRF/SA method with various preprocessing algorithms, such as median filter, histogram equalization, and CLAHE (Contrast Limited Adaptive Histogram Equalization). MRF/SA without any filter and contrast enhancement was also performed. A total of 210 mammograms with normal and abnormal findings were used. Abnormal category means mammogram with abnormalities findings whether in a form of benign lesion, malignant lesion, benign microcalcification or malignant microcalcification. ROC (Receiver Operating Characteristic) analysis was used to measure methods' performance. The values of area under the ROC curve (AUC) for MRF/SA only, median filter + MRF/SA, histogram equalization + MRF/SA and CLAHE+ MRF/SA are 0.731, 0.840, 0.798, and 0.746 respectively. Combination of median filter+ MRF/SA has the highest AUC value indicated that this method has the best performance in distinguishing normal and abnormal images. Histogram equalization+ MRF/SA has inferior AUC value compare to median filter + MRF/SA, but this combination has the highest sensitivity, 90.4%. This result shows that histogram equalization+ MRF/SA is the most successful method in detecting abnormal images correctly.

Keywords: *image segmenation, median filter, histogram equalization, CLAHE*

1. Introduction

Breast cancer is the second largest cancer prevalence among Indonesian women.¹ Currently, mammography is the most effective technique to detect breast abnormalities.² In most cases, mammograms are evaluated by radiologists to determine whether or not it shows cancerous appearance. Breast tumor detection performed by an experienced radiologist, however, can miss 10%-30% of breast cancer³ with the sensitivity of radiologist in detecting breast cancer being only 75%.⁴ Computer Aided Diagnosis (CAD) had been developed to increase the accuracy of mammography.⁵ The CAD system had been proven as a reliable, accurate, and efficient second reader.⁶ The CAD system improve the sensitivity of radiologists' performance from 73.5% to 87.4%. It also improves radiologists' specificity from 31,6% to 41.9%.⁷ The sensitivity of CAD system in detecting micro calcification is 99%, while its sensitivity for detecting masses is reported to be around 75%.⁸

Image segmentation is the most important part in CAD system⁹ being a process of parting image into homogeneous regions, separating the object of interest and the background.¹⁰ Image segmentation segments only the image without being able to recognize the segmented object.¹¹ Researches such as Byrd et al (2005)¹², Sheshadri et al (2005)¹³, Samma et al (2010)¹⁴ and Atlas et al (2014)¹⁵ developed CAD for mammography based on various kinds of image segmentation. Markov Random Field (MRF) is one of the promising methods in image segmentation,

especially for mammograms. MRF assumes that every pixel in image is connected to each other. To segment an image, this connection should be considered¹⁶, since it provides a good noise removal effect¹⁷ MRF had also proven its ability in producing good performance in image segmentation especially for objects with complex boundaries, image with a lot of noise¹⁸ and low contrast image such as MR brain scans.¹⁹ The quality of MRF segmentation has also been tested in mammography phantom (CDMAM). Iterative-based MRF gave a relatively better result in producing dot segments in the phantom matching its original's diameter with or without mammographic background.²⁰

Another component in CAD is the preprocessing stage. This stage usually performed by enhancing image's features, e.g. contrast and brightness, before entering the segmentation stage. The enhancement of a mammogram is very crucial since it yields supportive hands for diagnosis purpose.²¹ The result of image segmentation also depends on the preprocessing. Najdawi et al (2015) investigates various image enhancement algorithms and the combination to enhance the performance of mammogram segmentation. Contrast Limited Adaptive Histogram Equalization (CLAHE), median filter, and Gaussian smoothing are algorithms used in the research. Najdawi et al. concluded that the combination of CLAHE and median filter produces better segmentation result.

2. Materials and methods

2.1. Materials

There are 210 digital images with normal and abnormal findings used in this research. Abnormal image means mammogram with abnormalities whether in a form of benign lesion, malignant lesion, benign microcalcification or malignant microcalcification. Both images form Cranio Caudal (CC) and Medio Lateral Oblique (MLO) views were used. A total 40 images used as database, while the other 170 images used as the testing data. The database, consists of 20 images with abnormal diagnosis and 20 images with normal diagnosis, is used to observe segments' characteristics found in the normal and abnormal images. The observation result then tested on the 170 images in testing data. All the digital images along with the diagnosis were taken from Dharmais Hospital (National Cancer Center). The CAD program was developed using MatLab 2013 a software. Variety of preprocessing algorithms, such as CLAHE, median filter, and histogram equalization were also used to determine which algorithm giving the most satisfying result when combined with MRF.

2.2. Methods

The CAD system proposed in this work is based on Markov Random Field (MRF) image segmentation, being intended for mammography images. The MRF method is optimized with Simulated Annealing technique. All the results are evaluated visually by searching for clusters with certain pixel value and shape. The steps of this research are shown in Figure 1.

2.2.1. Preparation

All the mammograms obtained came with DICOM format and a uniform 2800×3506 size. In order to erase the metadata that contains patients' identity in the DICOM file, all the images were converted to .tiff format. This conversion also simplified the evaluation process which was performed visually.

The next step was the elimination of the black background in the image. This step was performed by cropping the image, leaving only the breast part and small part of the background. Afterwards, each image will have different size which depends on the breast size. Specific to the images taken from MLO position, removal of pectoral muscle was also performed. Pectoral muscle has high density, appearing as a large segment with high pixel value in the image. This appearance biases detection process that usually focus on segments/clusters with high pixel value.²²

2.2.2. Preprocessing

In this stage, all the images (database and testing data) were processed with 4 different procedures. The procedures involve three preprocessing algorithms; histogram equalization, median filter, and CLAHE. In the first procedure, images proceed directly to the segmentation process without any preprocessing. The second procedure was to process the images with histogram equalization prior to the segmentation process. The third was to have images filtered with

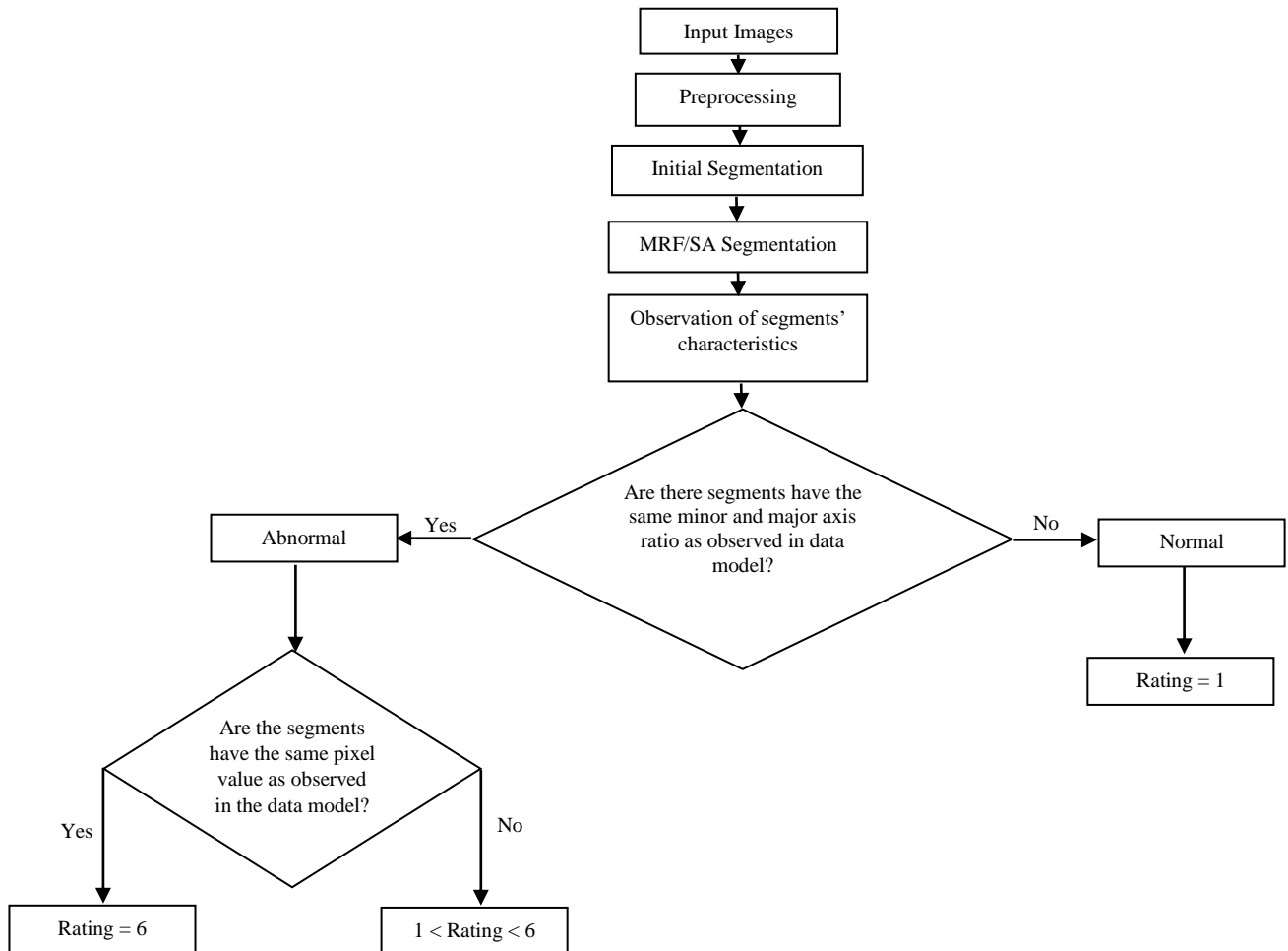


Figure 1. Work steps' chart.

median filter before the segmentation process. The last procedure was to apply CLAHE to the images first, before proceeding to segmentation process.

2.2.3. Segmentation

Segmenting an image can be seen as a labeling task. After this process, each pixel in the image will have a new label. Pixels with the same label imply that they belong to the same cluster/segment. There are two steps at this stage, the initial segmentation and the main MRF segmentation.

Initial segmentation

The aim of the initial segmentation step was to find the appropriate number of label for each image and to assign the initial label on image's pixels. Initial segmentation was achieved by finding minimum points at image's histogram (histogram valley) and multilevel thresholding. Histogram's minimum points were used to find the number of label and the initial label. Each image will have different number of labels/clusters due to different shape of histograms. In Figure 2b there are 8 minimum points on the histogram, meaning that there are 9 labels/clusters in the image. Multilevel thresholding process was performed to initially label each pixel with thresholding method. The pixel values at the minimum points were used as threshold value in multilevel thresholding.

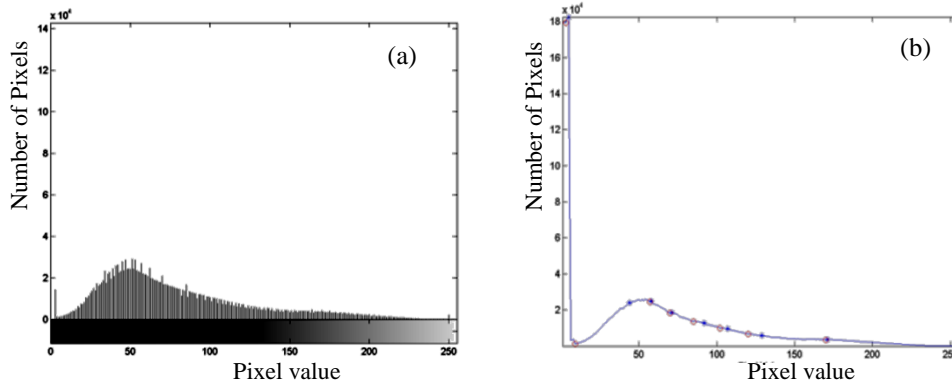


Figure 2. Finding histogram minimum points. (a) Original histogram and (b) minimum points of the histogram.

Main segmentation

After initial segmentation step, all images are segmented with Simulated Annealing optimized MRF. In segmenting an image, MRF considered two things; pixel value and connection between neighboring pixels. Suppose pixel x in image S has pixel value of f_x , and there is a label collection Ω that need to be assigned to image S so that pixel x labeled as ω_x ($\omega \in \Omega$), is having a range of possibility on label combinations to each pixel in image S . To estimate the most possible label, MAP (Maximum A Posteriori) estimator is the most commonly used estimator.²³ The estimator equation is²⁴:

$$\hat{\omega} = \arg \max \left\{ -\frac{(f - \mu_{\omega_x})}{\sigma_{\omega_x}} - \frac{1}{2} \log(2\pi\sigma_{\omega_x}^2) - U(\omega_x) \right\} \tag{1}$$

The minus sign in equation (1) can be eliminated, so the equation reads²⁴

$$\hat{\omega} = \arg \min \left\{ \frac{(f - \mu_{\omega_x})}{\sigma_{\omega_x}} + \frac{1}{2} \log(2\pi\sigma_{\omega_x}^2) + U(\omega_x) \right\} \tag{2}$$

The first two notations in equation (2) is Gaussian distribution that represents the first MRF consideration in image segmentation, which is the pixel value distribution in image. Meanwhile, energy function $U(\omega_x)$ is Gibbs energy which is the sum of all clique potential. Clique is a subset from pixels in image S that is a neighbor to each other. Gibbs energy represents the second consideration of MRF, neighboring pixels connection.

In Simulated Annealing optimization, temperature (T) variable is added in the process of finding the solution. The process starts from a state where all configurations have the same probability (high temperature). The cooling process represents the process of finding a solution that is done iteratively, where every iteration stated the temperature level of annealing process. The final equation used to find label for each pixel is¹⁶:

$$\hat{\omega} = \frac{\left(\log \sigma_{\omega_x} + \frac{(f_{\omega_x} - \mu_{\omega_x})}{\sigma_{\omega_x}} + U(\omega_x) \right)}{T} \tag{3}$$

2.2.4. Evaluation

Database observation

The initial step for this process was performed by observing all clusters present in database images and the properties of each clusters. There are two main properties observed, clusters' mean pixel value and shape. Region with abnormalities appears brighter than other region in mammogram. Therefore, abnormal clusters' tend to have the highest pixel value range in image.²⁵ However, high pixel value does not specifically signify abnormalities. The shape of abnormal masses can be round, oval, lobular and irregular.²⁶ If cluster with high pixel value has elongated shape, the cluster is most likely just a blood vessel. Blood vessel, veins and arteries can be seen in mammograms. Early calcification or arteries, along with twisted and overlapped blood vessel could mimic the appearance of malignant calcification.²⁷ Therefore, there are two parameters used to identify abnormal clusters, pixel value and clusters' shape. To accomodate the clusters' shape, the ratio of minor and major axis was used.

Testing data examination

In this process, clusters in the testing images were extracted. Then, the clusters were examined whether they meet the axis ratio and the pixel value from the observation result or not. The next step was to give rating 1 to 6 depends on findings in each testing images. Rating 6 means CAD system was sure that the image contains abnormalities, while rating 1 means CAD system was sure that the image was normal. If the testing images contain clusters that meets axis ratio and pixel value from the observation result, rating 6 was given. If no cluster meets any of the criteria from observation result, rating 1 was given. If cluster meets the axis ratio criteria but didn't meet the pixel value criteria, $1 < \text{rating} < 6$ was given, depend on how close the pixel value of the cluster to the one in observaton result.

ROC calculation

Based on the rating of the testing data, Receiver Operating Characteristic (ROC) was calculated. This process included the accuracy, sensitivity, and specifity calculation, ROC curve drawing along with the AUC (Area Under ROC curve) score. The accuracy score indicatethe overall performance of the method, while sensitivity and specifity score shows the method's performance in detecting abnormal and normal images, respectively. The AUC score indicates how well a method in distinguishing normal and abnormal images. AUC score below 0.5 means the method has a poor performance.

3. Results and Discussion

Table 1 shown the pixel value range and axis ratio of abnormal clusters obtained from the database. Contrast enhancement (histogram equalization and CLAHE) + MRF/SA method generates a slightly different pixel value range. Median filter + MRF/SA and MRF/SA only has the same pixel value range. Unlike filtering algorithm, contrast enhancement works by changing the distribution of pixels the histogram. This equalization process changes the distribution of pixels in histogram bins, causing certain pixel values have more pixels than other. This led the abnormal clusters to have a different pixel value range with the original one.

Table 1. Pixel value range of abnormal clusters.

Methods	Pixel value range	Minor and mayor axis ratio
MRF/SA only	215-255	0.49-1.00
Histogram equalization + MRF/SA	212-255	0.46-1.00
Median filter + MRF/SA	215-255	0.49-1.00
CLAHE + MRF/SA	218-255	0.46-1.00

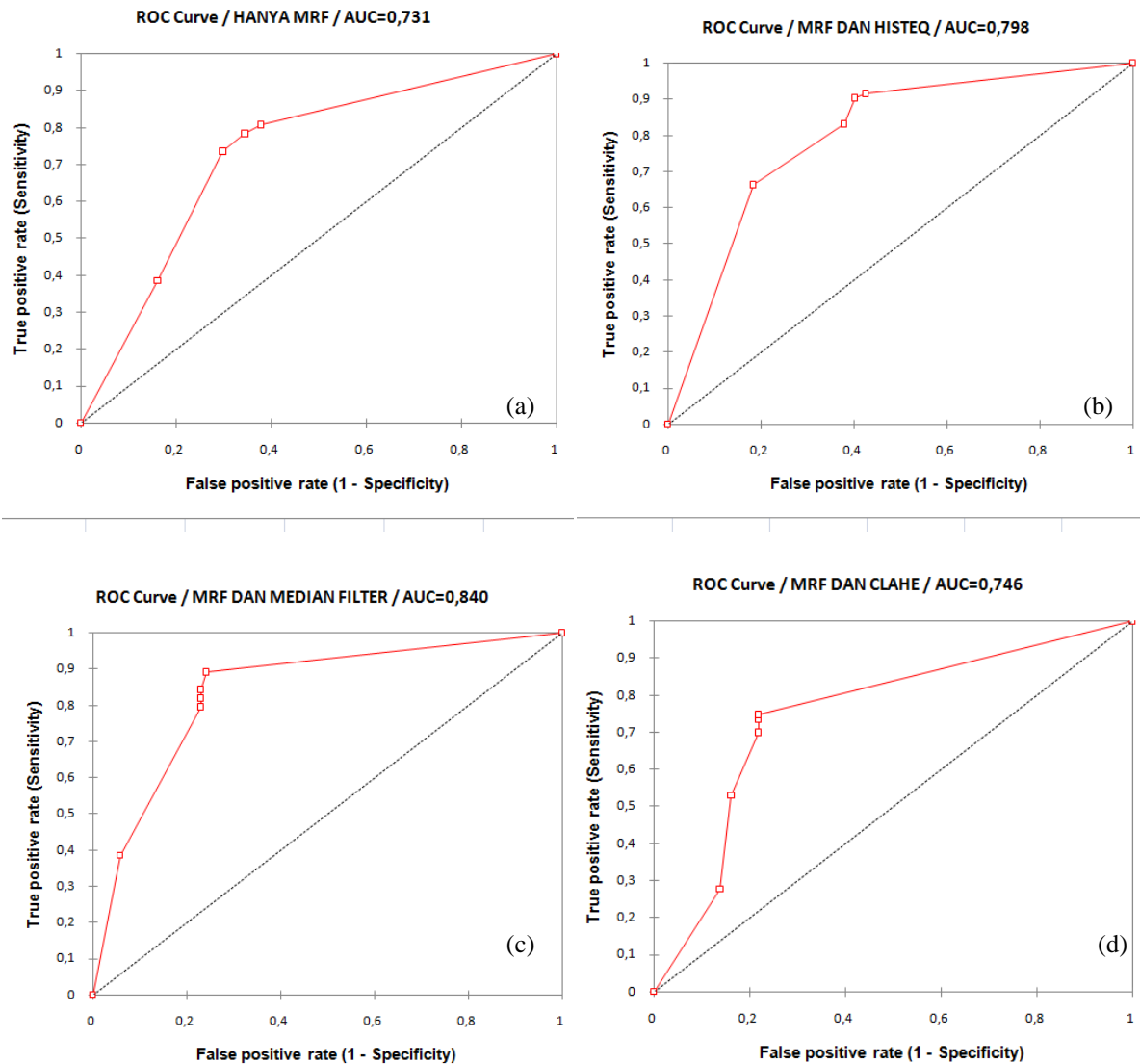


Figure 3. Receiver Operating Characteristic (ROC) Curve. (a) MRF/SA only, (b) Histogram equalization + MRF/SA, (c) Median filter + MRF/SA, (d) CLAHE + MRF/SA.

Based on the evaluation results of MRF with 4 different preprocessing, it turned out that every combination has different superiority. The results of performance measurement are shown in Table 2. The ROC curves are shown in Figure 3.

From Table 2, it can be observed MRF only method that has the lowest accuracy and AUC score. It means MRF only method has the worse performance in differentiating normal and abnormal images. This result also indicates the importance of preprocessing stage (filtering and contrast enhancement) in image segmentation. Mammogram has low contrast and contains high level of noise. Low contrast causes the abnormal clusters and surrounding area to have similar properties, making them difficult to segment. Noise existence that usually in the form of high pixel value dots, causing many normal images to be classified as abnormal.

Table2. The results of performance measurement.

Measurements	MRF/SA only	Histogram equalization + MRF/SA	Median filter + MRF/SA	CLAHE + MRF/SA
Accuracy	78.1%	74.7%	82.4%	76.5 %
Sensitivity	78.3%	90.4 %	89.2%	74.7%
Specifity	65.5%	59.8%	75.9%	78.2%
AUC Score	0.731	0.798	0.840	0.746

CLAHE + MRF/SA method has the highest specificity but the lowest sensitivity. The specificity scores shows that this method excels in detecting normal image, while the low sensitivity indicates that this method also detects a lot of abnormal images as normal. Pixels' distribution in mammogram fulfilled a Gaussian distribution where low pixel values and high pixel values have lower number of pixels than the medium pixel values (Figure 4a). CLAHE modifies histograms so that pixels distributes equally (Figure 4b) and causes every pixel value to have almost the same amount of pixels.

The process of finding number of clusters in an image was performed by counting number of histogram's minimum points as seen in Figure 2, so the shape of histogram is important. Histogram modification performed by CLAHE yields in a flat histogram. Therefore irregular number of clusters found in image and generates undersegmented or oversegmented images that caused many abnormal images detected as normal. In an undersegmented image, where only small number of clusters found, the size of each cluster became larger and the pixel value range represented by each cluster became wider, making it challenging to distinguish the abnormal clusters. The oversegmented image, which has lots of clusters found, caused the size of each cluster is too small, so it is difficult to evaluate the shape of the cluster visually.

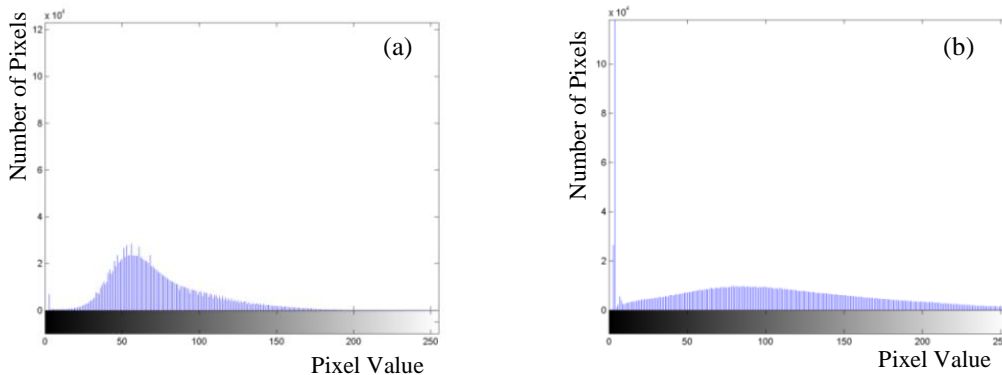


Figure 4. CLAHE equalization. (a) Original histogram and (b) histogram after CLAHE applied.

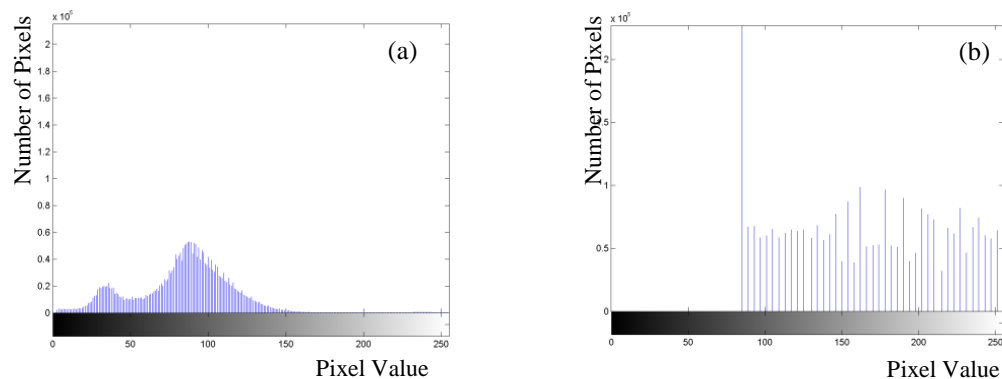


Figure 5. Histogram equalization. (a) Original histogram and (b) histogram after histogram equalization applied.

Histogram equalization+ MRF/SA has the highest sensitivity but the lowest specificity. These scores show that this method excels in detecting abnormal images but also detects many normal images as abnormal. Although histogram equalization works in an almost similar way to CLAHE, as a contrast enhancement, histogram produced by histogram equalization was not as flat as those of CLAHE's, as seen in Figure 5. The minimum points of histogram, which were used to find number of clusters, can still be distinguish clearly, so there weren't any oversegmented and undersegmented image found. But, this algorithm redistributes pixels to higher pixel value area. As number of pixels with high pixel values increase, the abnormal clusters, which have high pixel value, are now more visible, since more pixels are added to the cluster. In the other hand, the pixel value of normal clusters was also shifted. Normal clusters, which initially have low pixel value, now has high pixel value due to the pixel's redistribution performed by histogram equalization. This caused many abnormal clusters were detected in normal images. This detection may become a false alarm as well as a reference to radiologist to pay more attention in those clusters.

From Table 2, median filter + MRF/SA method has the highest accuracy and AUC score. Those results indicated that this method was the best method to distinguish normal and abnormal images. Median filter works by removing noise in image while still preserving the edges of the object. Noise that usually appears in a high pixel value form has been removed, so there are no high pixel valued clusters detected as abnormal clusters found in normal image. On the other hand, the edges of abnormal clusters are still maintained, so the abnormal clusters are easily distinguishable from the surroundings.

Figure 6 shows abnormal images. Clusters with high pixel value are shown in maroon color. Images obtained from histogram equalization + MRF/SA method (Figure 6c) and median filter+MRF/SA method (Figure 6d) shows maroon clusters that fulfilled the pixel value and axis ratio criteria as in Table 1, therefore rating 6 was given. Based on the cluster's shape, clusters that fulfilled axis ratio criteria has an un-elongated shape as seen in Figure 6c and 6d. MRF only method (Figure 6b) shows some small maroon clusters. One of the cluster has axis ratio of 0.55, so it meets the axis ratio criteria of abnormal cluster. But that cluster has pixel value of 191, so rating 5.7 was given. In the other hand, CLAHE+MRF/SA method generates an undersegmented image as shown in Figure 6e. There are only three segments in the image, a large sized maroon cluster, a green segment in background of the breast, and a blue segment as the background of the image, so the real abnormal region could not be observed clearly. Rating 1 was given to Figure 6e.

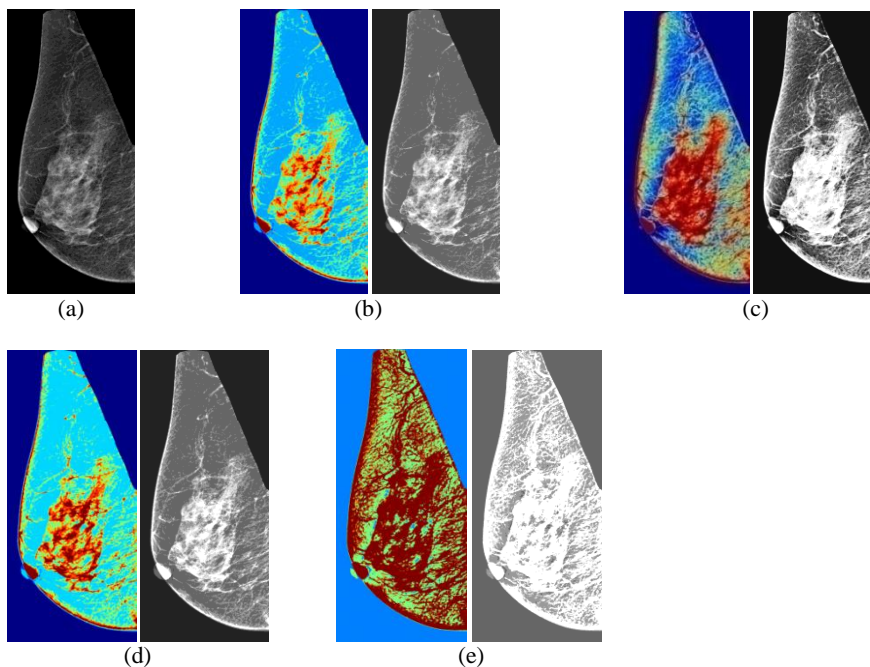


Figure 6. Example of abnormal image. (a) original image, (b) image after MRF/SA only process, (c) image after histogram equalization +MRF/SA process, (d) image after median filter+MRF/SA process, (e) image after CLAHE+MRF/SA process.

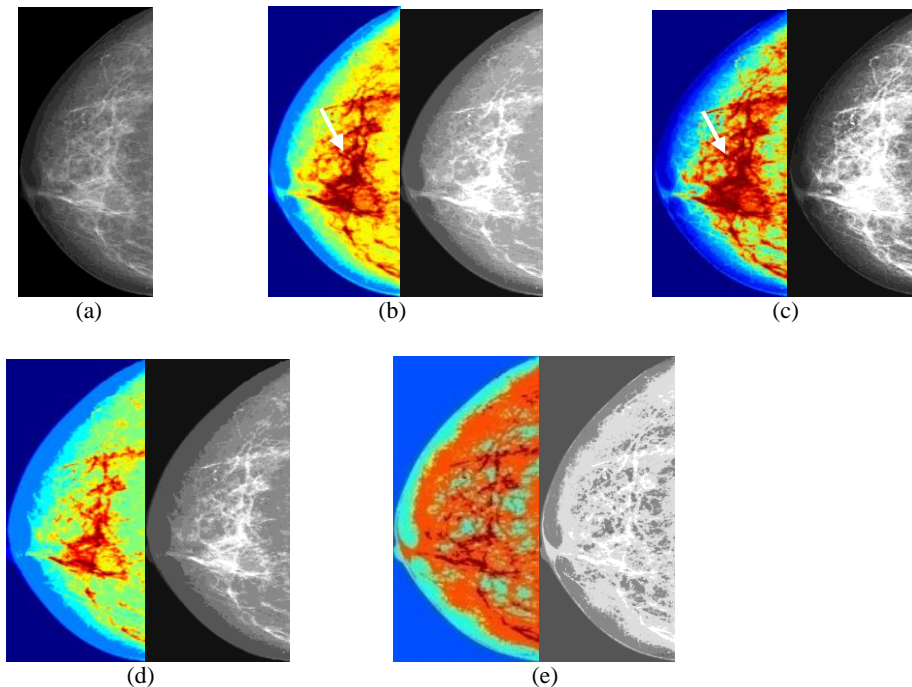


Figure 7. Example of normal image (a) original image, (b) image after MRF/SA only process, (c) image after histogram equalization + MRF/SA process, (d) image after median filter + MRF/SA process, (e) image after CLAHE + MRF/SA process.

Example of normal images shown in Figure 7. Abnormal clusters were detected by MRF/SA only method and histogram equalization + MRF/SA method. Maroon clusters pointed with white arrow in Figure 7b and 7c are the abnormal clusters detected by the methods. The pixel value and shape of those clusters were fulfilled the pixel value and axis ratio criteria in Table 1, so rating 6 was given. It can be seen that those clusters are slightly larger than other cluster with the same color. This result was contrary to the radiologist diagnosis that stated the image was normal.

The superiority of median filter+MRF/SA method and CLAHE+MRF/SA method in detecting normal image shown in Figures 7d and 7e. It can be seen that the maroon clusters in those figures are elongated, they didn't meet the axis ratio criteria, so rating 1 was given.

4. Conclusion

Among four variety of combined MRF method, median filter+MRF/SA method is deemed the most accurate method in matching radiologist's diagnosis. Histogram equalization+MRF/SA method is the best method in detecting abnormal images as well as finding abnormal clusters in normal images. CLAHE+MRF/SA method is the best method in detecting normal images.

MRF segmentation method can be developed by combining the preprocessing methods. The combination of filtering and contrast enhancement in the preprocessing stage should be able to produce better segmentation result. Removing noise will reduce the possibility of method detecting normal image as abnormal. Enhanced contrast will also makes abnormal clusters clearly distinguishable.

References

- ¹ Kementrian Kesehatan RI Pusat Data dan Informasi Kesehatan, “Stop Kanker,” infodatin-Kanker hal 3 (2015).
- ² N. Al-Najdawi, M. Biltawi, and S. Tedmori, “Mammogram image visual enhancement, mass segmentation and classification,” *Appl. Soft Comput. J.* **35**, 175–185 (2015).
- ³ A. Wroblewska, “Segmentation and feature extraction for reliable classification of microcalcifications in digital mammograms,” *Optoelectronics* **11**(3), 227–235 (2003).
- ⁴ R.E. Bird, “Professional quality assurance for mammography screening programs,” *Radiology* **177**(2), 587 (1990).
- ⁵ K. Thangavel, M. Karnan, R. Sivakumar, and A.K. Mohideen, *Automatic Detection of Microcalcification in Mammograms - A Review* (2005).
- ⁶ M. Gromet, “Comparison of computer-aided detection to double reading of screening mammograms: Review of 231,221 mammograms,” *Am. J. Roentgenol.* **190**(4), 854–859 (2008).
- ⁷ Y. Jiang, R.M. Nishikawa, R.A. Schmidt, C.E. Metz, M.L. Giger, and K. Doi, “Improving breast cancer diagnosis with computer-aided diagnosis,” *Acad. Radiol.* **6**(1), 22–33 (1999).
- ⁸ L.J. Warren Burhenne, S. a Wood, C.J. D’Orsi, *et al.*, “Potential contribution of computer-aided detection to the sensitivity of screening mammography,” *Radiology* **215**(2), 554–562 (2000).
- ⁹ S. Loncaric, “Multiresolution simulated annealing for brain image analysis,” *Proc. SPIE* 1139–1146 (1999).
- ¹⁰ W.K. Pratt, “Image Segmentation,” *Comput. Vis.* 579–622 (2000).
- ¹¹ G. Dougherty, “Introduction,” in *Med. Image Process. Tech. Appl.*, edited by G. Dougherty (Springer New York, New York, NY, 2011), pp. 1–4.
- ¹² K. Byrd, J. Zeng, and M. Chouikha, “Performance assessment of mammography image segmentation algorithms,” in *34th Appl. Imag. Pattern Recognit. Work.* (2005), p. 6 pp.-pp.157.
- ¹³ S. Hs, “Detection of breast cancer by mammogram image segmentation,” **1**(4), 232–234 (2017).
- ¹⁴ H. Samma, C.P. Lim, and A. Samma, “A Computer-Aided Detection System for Automatic Mammography Mass Identification,” in *Neural Inf. Process. Model. Appl. 17th Int. Conf. ICONIP 2010, Sydney, Aust. Novemb. 22-25, 2010, Proceedings, Part II*, edited by K.W. Wong, B.S.U. Mendis and A. Bouzerdoum (Springer Berlin Heidelberg, Berlin, Heidelberg, 2010), pp. 226–233.
- ¹⁵ N. El Atlas, M. El Aroussi, and M. Wahbi, “Computer-aided breast cancer detection using mammograms: A review,” in *2014 Second World Conf. Complex Syst.* (2014), pp. 626–631.
- ¹⁶ O. Demirkaya, M.H. Asyali, and P.K. Sahoo, *Image Processing with MATLAB: Applications in Medicine and Biology* (Taylor & Francis, 2008).
- ¹⁷ Q. Dai, J. Qiao, F. Liu, X. Shi, and H. Yang, “A Human Body Part Segmentation Method Based on Markov Random Field,” *2012 Int. Conf. Control Eng. Commun. Technol.* 149–152 (2012).
- ¹⁸ J. Wu and A.C.S. Chung, “A segmentation model using compound Markov random fields based on a boundary model,” *IEEE Trans. Image Process.* **16**(1), 241–252 (2007).
- ¹⁹ B. Scherrer, F. Forbes, C. Garbay, and M. Dojat, “Distributed local MRF models for tissue and structure brain segmentation,” *IEEE Trans. Med. Imaging* **28**(8), 1278–1295 (2009).
- ²⁰ W.J. Veldkamp and N. Karssemeijer, “Accurate segmentation and contrast measurement of microcalcifications in mammograms: a phantom study,” *Med. Phys.* **25**(7 Pt 1), 1102–10 (1998).
- ²¹ S. Anand and S. Gayathri, “Mammogram image enhancement by two-stage adaptive histogram equalization,” *Optik (Stuttg.)* **126**(21), 3150–3152 (2015).
- ²² J. Nagi, S.A. Kareem, F. Nagi, and S.K. Ahmed, “Detection Using Digital Mammograms,” *IEEE EMBS Conf. Biomed. Eng. Sci.* (December), 87–92 (2010).
- ²³ S.Z. Li, *Markov Random Field Modeling in Image Analysis Third Edition* (n.d.).
- ²⁴ Z. Kato, “Markov Random Fields in Image Segmentation,” (2008).
- ²⁵ M.J. Yaffe, “Mammographic density Measurement of mammographic density,” **10**, 1–10 (2008).
- ²⁶ J. Mandell, *Core Radiology* (Cambridge University Press, 2013).
- ²⁷ M. Torosian, *Breast Cancer: A Guide to Detection and Multidisciplinary Therapy* (Humana Press, 2002).